NASA Technical Memorandum 101977
AIAA-89-2942

Investigation of Low NO_x Staged Combustor Concept in High-Speed Civil Transport Engines

Hung Lee Nguyen, David A. Bittker,
and Richard W. Niedzwiecki
Lewis Research Center
Cleveland, Ohio

Prepared for the
25th Joint Propulsion Conference
cosponsored by the AIAA, ASME, SAE, and ASEE
Monterey, California, July 10–12, 1989

NASA

INVESTIGATION OF LOW NO_x STAGED COMBUSTOR CONCEPT IN HIGH-SPEED CIVIL TRANSPORT ENGINES

Hung Lee Nguyen,* David A. Bittker,** and Richard W. Niedzwiecki†
National Aeronautics and Space Administration
Lewis Research Center
Cleveland, Ohio 44135

Abstract

The purpose of this report is to predict levels of exhaust emissions due to high temperatures in the main combustor of High-Speed Civil Transport (HSCT) engines during supersonic cruise. These predictions are based on a new combustor design approach: a rich burn/quick quench/lean burn combustor. A two-stage stirred reactor model is used to calculate the combustion efficiency and exhaust emissions of this novel combustor. A propane-air chemical kinetics model is used to simulate the fuel-rich combustion of jet fuel. Predicted engine exhaust emissions are compared with available experimental test data. The effect of HSCT engine operating conditions on the levels of exhaust emissions is also presented. The work described in this paper is a part of the NASA Lewis Research Center High-Speed Civil Transport Low NO_x Combustor program.

Introduction

The nitrogen oxide (NO_x) exhaust emissions of the High-Speed Civil Transport (HSCT) turbofan or turbojet engines at Mach 2.0 to 4.0 and high-altitude cruise may have detrimental effects on the stratospheric ozone layer.[1] The damaging effects of pollutants from exhaust emissions have been reported extensively elsewhere.[2-10] It is anticipated that current combustor designs operating in a high-speed propulsion system will produce nitrogen oxide levels that are much higher than in current subsonic applications.[2] HSCT stratospheric flight could produce detrimental climatic effects. Therefore, considerable research is needed to develop practical combustors with extremely low levels of NO_x emissions.

The main engine components of a (turbofan) turbojet include a fan (turbofan), a compressor, a combustor, and a turbine. A portion of the compressed air passing through the turbofan enters the compressor, while the remaining air is bypassed around the core engine to provide additional thrust. The flow rate and the total temperature and pressure of the compressed air entering the combustor from the compressor discharge are determined by the overall fan and compression ratio, flight altitude, and flight speed. The high Mach cruise operation mode of HSCT engines imposes increased pressures and temperatures at the inlet of the turbomachinery, and subsequently, much higher temperatures and pressures at the combustor inlet. The fuel-air ratio is determined by the combustor temperature rise required to obtain the design turbine inlet temperature. The maintenance of high-Mach flight requires considerable energy input, resulting in very high turbine inlet temperatures and therefore, high fuel-air ratios. Table I shows a comparison of typical cruise operating conditions for a conventional subsonic application and an HSCT together with their expected NO_x emission levels. The effect of the combustor in HSCT engines (i.e., combustor inlet and exit temperatures and combustor inlet pressure) on NO_x emission levels is of particular importance.

The two principle methods for controlling NO_x formation are (1) reducing the reaction-zone temperature (flame temperature) and (2) reducing the reaction-zone residence time. The reaction-zone temperature may be reduced by operating with either a fuel-rich[11-15] or fuel-lean reaction zone,[16-20] by operating with a more homogeneous fuel-air mixture, or by introducing inert substances into the reaction zone. The reaction-zone fuel-air ratio may be shifted by altering the combustor airflow distribution. However, a rich zone tends to form considerable amounts of carbon monoxide, hydrocarbons, and soot, while lean reaction zones pose severe combustion stability problems. Variable geometry might be required to continuously control combustor airflow distribution for a wide range of engine operating conditions from light-off through idle to low and intermediate power to high-power cruise conditions.[21]

The fuel-air mixture could be made more homogeneous by increasing mixing intensity, by using a very large number of fuel injection points to distribute the fuel uniformly, and possibly by close coupling with a flame holder to provide high turbulence for rapid mixing. Premixing the fuel and air before they enter the reaction zone also produces more uniform fuel-air mixtures in the reaction zone;[22-25] however, premixing might be impractical because fuel autoignition or flashback is likely to occur with the severe cycle conditions associated with an HSCT engine. Prevaporizing the fuel before it enters the reaction zone also helps to achieve a uniform fuel-air mixture;[26] but fuel autoignition or flashback is also likely to occur in the prevaporizing process. Flame temperature, and the likelihood of autoignition or flashback, could be reduced by inert substances such as water or recirculated combustion products.[27] Unfortunately, water injection would be impractical during cruise because of payload penalties, and a significant increase in the amount of combustion products recirculated in the reaction zone might require excessive pressure losses. The reaction-zone residence time could be reduced either by shortening the length of the reaction zone or by increasing the number of local burning zones to reduce the recirculation path length.

The abatement of NO_x emissions to low levels at HSCT cycle conditions will require nearly perfect mixing, reduction of flame temperature, and

*Aerospace engineer.
**Research scientist.
†Chief, Combustion Technology Branch.

reduction of residence time. Most of the extensive previous work directed at controlling NO_x emissions in subsonic engines[18-27] is likely to be of only limited use at the cycle conditions envisioned for an HSCT. The purpose of this investigation is to provide an important initial step in the design of combustors aimed at limiting NO_x emissions in HSCT engines. One low NO_x combustor concept is the rich burn/quick quench/lean burn combustor. This air-staged combustor consists of a rich primary stage followed by a quick-quench mixer that dilutes the fuel-rich primary products for introduction to a fuel-lean stage for final consumption of the fuel. This combustor concept is intended to partially burn the fuel-air mixture in the oxygen-deficient primary zone, where the combustion temperature is lower, to minimize the formation of NO_x emissions. The exiting, hot fuel-rich mixture is then quickly and uniformly quenched so that a minimum of thermal NO_x will be formed in the final short-lean reaction zone.

The objective of this investigation is two-fold. First, the combustion chemical kinetics of propane-air were developed at fuel-rich conditions and lower temperatures and pressures. The calculated results were then compared with available experimental data of the rich burn, quick quench, lean burn combustion system. Second, the effect of HSCT engine operating conditions in controlling NO_x emissions in the rich burn/quick quench/lean burn combustor were investigated.

Description of Models

Multistage Well-Stirred Reactor Model

The stirred-reactor calculations presented in this report were made with the computer program described in references 28 and 29. A well-stirred reactor consists of a combustion chamber with a well-defined volume into which the fuel-air mixture enters and instantaneously mixes with the reactor contents at a constant pressure. The mixture of reactants and products flows out continuously in a manner which results in a steady-state operation. The conservation equations for mass, species, and energy form a system of nonlinear algebraic equations that were solved by a modified Newton-Raphson iteration procedure. No heat transfer losses were considered in the model. The exhaust gases from the primary-stage reactor were assumed to be instantaneously diluted with the required amount of air and then to enter the second-stage reactor. The turbulent mixing between the end of the primary combustion zone and the start of secondary combustion was approximated by the back-mixing of the fuel-air mixture in the model.

Chemical Kinetic Model

The chemical kinetic reaction model and the rate coefficients for propane-air combustion and NO_x formation used in this study are listed in Table 2. This mechanism is an improved version of the mechanism used by Bittker and Wolfbrandt to model similar rich-lean propane-air combustion in a two-stage flame tube.[14] Additional reactions involving H-O-N species have been added and the rate coefficients have been updated by using the recent literature.[30-41] It is recognized that the oxidation mechanism of propane and the formation mechanisms of NO and NO_2 (NO_x) are not known with great certainty, especially at rich equivalence ratios. Soot formation in rich hydrocarbons combustion is also a complicating factor. For these preliminary idealized computations, to investigate the rich burn/quick quench/lean burn concept of NO_x control, we have used the simplified well-stirred reactor model and have neglected any effects of soot formation. The chemical model went through several iterations until we found one that could be verified by available experimental data. A description of this model follows.

Reactions (1) to (3) (Table 2) describe the formation of nitric oxide according to the extended Zeldovich mechanism, and reaction (4) describes the formation of atomic nitrogen which has been found to be important for rich mixtures. Other reactions concerning the formation of NO_x are described by reactions (5) to (34). Reactions (35) to (102) describe the oxidation of propane and the formation of the hydrocarbon fragments. The reactions involving hydrocarbon fragments and NO are described by reactions (5) to (6). In addition, the reactions between H_2O and the radicals H, O, and OH and the conversion of NO to nitrogen dioxide, NO_2, are also included.

Table 3 lists third-body collisional recombination reactions[14] together with the chaperon efficiency factors for several third-body species used in the chemical kinetics model.

Validation of Models

The propane-air mechanism was tested by repeating the computations of Bittker and Wolfbrandt[14] which modeled the experimental NO_x and CO measurements of G. Wolfbrandt and D. Schultz.[42] Their experimental work was undertaken as part of the Critical Research and Technology program funded by the Department of Energy. The purpose was to determine the effect of combustion operating conditions on the conversion of fuel-bound nitrogen to nitrogen oxides. Wolfbrandt and Schultz employed a two-stage flame tube using propane-air and propane-toluene-air mixtures. Pyridine was added to simulate fuel-bound nitrogen.

Figure 1 compares computed and experimental NO_x concentrations for a range of primary equivalence ratios from 0.6 to 1.8. Secondary air was added to give a secondary equivalence ratio value of 0.5. The primary-zone and secondary-zone residence times were kept at nominally 11 and 2 msec, respectively. The inlet air temperature was 672 K and the reactor pressure was kept at 5 atm. The results are for a propane-air mixture with no added fuel-bound nitrogen.

Figure 2 compares experimental and computed CO concentrations for the same operating conditions given in Fig. 1. Good agreement between experimental and computed results is obtained for both pollutants. The extended propane-air combustion and NO_x formation mechanisms used in the present work give better agreement between experimental and computed pollutants measurements than those obtained from previous studies.[14] The effects of various operational parameters on pollutant emissions of HSCT engines are discussed next.

Results and Discussion

Effect of Primary-Zone Residence Time

Previous work on the low NO_x rich burn/quick quench/lean burn combustor from the DOE/NASA Low NO_x Heavy Fuel Combustor Concept Program[11] indicated that film cooling, if used, would produce copious amounts of thermal NO_x in the rich zone. Therefore, the rich primary zone was totally regeneratively convectively cooled. It became clear that for a rich primary zone to function successfully, there must be circumferentially uniform, effective convection cooling of the liner wall. The overheating of the liner wall in the rich zone could limit the operating conditions to a lower inlet air temperature. Thus, a rich primary zone with smaller dimensions would improve the combustor durability. Furthermore, the overall length of the combustor should be kept as short as practical to minimize engine shaft length and bearing requirements and to meet space limitations of HSCT engines and the fuselage area.

Calculations were carried out for the rich burn/quick quench/lean burn combustor to study the effect of primary-zone residence time on pollutant emissions. The effect of a smaller, rich primary zone on pollutant emission are shown in Figs. 3 to 5. Primary-zone residence time is varied by changing the rich primary-zone reactor volume. The NO_x concentration decreases as primary-zone residence time decreases for both primary-zone equivalence ratios. A comparison of Fig. 4 with Fig. 3 indicates that the NO_x results are more sensitive to primary-zone residence time variation for high inlet temperatures and pressures. These results are explained by the temperature, pressure, and residence time effects on NO_x forming reactions as discussed in the previous section. The CO concentration also decreases noticeably as primary-zone residence time decreases at high inlet temperatures and pressures (Fig. 5).

Effect of Secondary-Zone Residence Time

The effect of lean secondary-zone residence time on NO_x and CO concentrations is shown in Figs. 6 and 7, respectively. Figure 6 shows that the NO_x emissions are sensitive to variation of residence time in the lean secondary zone. There is a 36 percent decrease in NO_x concentration as secondary residence time decreases from 2.8 to 0.9 msec. This decrease is due to the shorter amount of time available at the burning conditions. In contrast, the CO concentration increases by 45 percent as the secondary-zone residence time decreases from 2.8 to 0.9 msec (Fig. 7). The decrease in reaction time in the lean zone suppresses the CO reaction and results in higher CO levels in the combustor exhaust.

Effect of Primary-Zone Equivalence Ratios

The purpose of these parametric tests was to assess the effects of varying primary-zone equivalence ratio. The rich primary-zone equivalence ratios were varied from 1.0 to 2.0. A comparison of NO_x emissions at each inlet air temperature is given in Fig. 8 for an initial pressure of 7.6 atm. The observed NO_x values generally are highest at an equivalence ratio of about 0.9 or 1.0, and the minimum NO_x levels usually occur between rich primary-zone equivalence ratios of 1.5 and 1.7. Minimum NO_x emissions occurred at a rich primary-zone equivalence ratio of 1.6 for all of the test cases studied. These data indicate that the minimum NO_x is below 800 ppmm for the highest inlet air temperature of 1311 K. The operating conditions of the reactors together with the variation of NO_x emissions with primary-zone equivalence ratio at each inlet air temperature are summarized in Table 4.

It has been postulated and later demonstrated in fundamental experiments that a fuel-rich combustion zone can be effective in suppressing NO_x formation[13,15] because oxygen is unavailable. The absence of oxygen in the fuel-rich zone is clearly illustrated in Fig. 9. The ability of the rich burn/quick quench/lean burn combustor to achieve similar low NO_x point and levels with significantly different inlet air temperature conditions is clearly demonstrated in Fig. 8.

The primary-zone equivalence ratio was also varied from 0.6 to 0.8 to show the variation of NO_x emissions with the lean primary-zone equivalence ratios (Fig. 8). A lean primary zone operates at lower reaction temperatures than a rich primary zone. This is clearly illustrated in Fig. 10. Therefore, the volume required for the lean primary zone is larger than the rich primary-zone section. In general, NO_x is formed when nitrogen in the atmosphere is subjected to high temperatures over a finite period of time in the presence of oxygen. The oxidation of atmospheric nitrogen can be minimized by operating at reaction-zone temperature levels below approximately 1644 K. Unfortunately, in the excess oxygen state of lean combustion, atmospheric nitrogen can still react to produce high levels of NO_x. This would explain the higher NO_x levels obtained at a primary-zone equivalence ratio of 0.8 compared to the NO_x levels obtained at a primary-zone equivalence ratio of 1.2. This increase in NO_x levels is more pronounced as the inlet air temperature increases as illustrated in Fig. 8.

Table 5 summarizes CO emissions results as a function of rich and lean primary-zone equivalence ratios. Figure 11 shows CO emissions for nine different primary-zone equivalence ratios having lines of constant inlet air temperatures. As primary-zone equivalence ratio increases, CO emissions increase proportionally. Apparently, if the low NO_x and CO goals were achieved simultaneously, the minimum NO_x achieved might be compromised. If the need to reduce CO becomes important, the rich primary-zone stoichiometry should be leaned to the 1.4 to 1.5 equivalence ratio range to produce less CO while accepting some increase in NO_x emissions. Emissions results for CO_2 as a function of primary-zone equivalence ratio and inlet air temperature are shown in Table 6. The high concentration of CO_2 emissions indicates that most CO was oxidized. The unburned hydrocarbon emissions (C_3H_8, CH_4, C_2H_4, and C_2H_6) were at extremely low concentrations at all conditions studied. These unburned hydrocarbon emissions are the same as the unburned hydrocarbon concentrations obtained from equilibrium combustion calculations.

Effect of Inlet Air Temperature

A series of parametric tests was carried out to evaluate the sensitivity of the rich burn/quick

quench/lean burn combustor exhaust emissions to inlet air temperatures. NO_x emissions levels are summarized in Table 4 and shown in Fig. 8 as a function of inlet air temperature. NO_x emissions appear to vary exponentially with changes in inlet air temperature. Figure 8 shows that the NO_x minimum increases 620 ppmm for a 311 K increase in inlet air temperature. A higher inlet air temperature causes higher reaction temperatures in the lean secondary zone (Fig. 12). This results in higher NO_x emissions in the combustor exhaust.

The effects of inlet air temperature on CO emissions are summarized in Table 5 and shown in Fig. 11. Changes in combustor inlet air temperature have a smaller observable effect on CO emissions, especially at the higher equivalence ratio limit of the primary-zone stoichiometry. The decrease in the availability of oxygen due to the increase in the primary-zone equivalence ratio decreases the CO reaction rate and does not produce an observable effect on CO emissions by inlet air temperature at high primary-zone equivalence ratios. Table 6 summarizes how CO_2 emissions change as inlet air temperatures are raised.

Effect of Initial Pressure

The effect of pressure on exhaust emissions was also studied (Figs. 13 and 14). The pressure variation was 7.6 to 16 atm, the combustor inlet air temperature was 1311 K, and the lean secondary-zone equivalence ratio was 0.5. Primary-zone equivalence ratios again ranged from 0.6 to 2.0. The data indicated that increasing the pressure causes an increase in both NO_x and CO emissions levels. However, the increase in NO_x levels due to pressure is smallest at the minimum NO_x points. This again illustrates the ability of the rich burn/quick quench/lean burn combustor to achieve similar low NO_x levels even when initial pressure conditions vary significantly.

Effect of Secondary-Zone Equivalence Ratios

The effect of lean secondary-zone equivalence ratios on emissions was studied by varying them from 0.5 to 0.7. Figure 15 shows NO_x emissions for three different lean secondary-zone equivalence ratios. The NO_x emission increased by 79 percent as the lean-zone equivalence ratio was varied from 0.5 to 0.7. Change in the lean-zone equivalence ratio also had an observable effect on CO emission. Figure 16 indicates that CO emission increased by 62 percent as the lean secondary-zone equivalence ratio was varied from 0.5 to 0.7. The higher availability of oxygen in the lean zone at lower equivalence ratios increases the CO reaction rate and results in lower CO in the combustor exhaust.

Conclusions

The effects of HSCT operating conditions on exhaust emissions of the rich burn/quick quench/lean burn combustor were studied. Experimental data[14] were compared with calculated results. The major conclusions drawn from this study follow:

1. For the most severe operating conditions considered (combustor inlet temperature, 1311 K; combustor inlet pressure, 16 atm), the combustor produces NO_x emissions of 850 ppmm at the minimum in the NO_x curve in the region of the 1.6 primary-zone equivalence ratio. The level of CO emissions was below 670 ppmm at these operating conditions. Unburned hydrocarbons were very minimal at all conditions tested.

2. At the optimum configuration for minimum NO_x, the rich burn/quick quench/lean burn combustor shows only small increases in NO_x emission levels as the combustor inlet temperature and pressure are increased. The minimum in the NO_x curve does not change with variations in combustor inlet temperature and pressure. This demonstrates the ability of the rich burn/quick quench/lean burn combustor to suppress NO_x emissions.

3. NO_x emissions vary directly with changes in combustor initial inlet air temperature, pressure, rich primary-zone and lean secondary-zone residence time, and lean secondary-zone equivalence ratio.

4. CO emissions vary in a direct manner with changes in combustor initial inlet air temperature, pressure, rich primary-zone residence time, and lean secondary-zone equivalence ratio. They vary in an inverse manner with changes in the lean secondary-zone residence time.

References

1. Broderick, A.J., ed., "Nature of Propulsion Effluents," Climatic Impact Assessment Program, Vol. II, DOT-TSC-OST-73-4, U.S. Department of Transportation, Mar. 1973.

2. Strack, W.C., "Propulsion Challenges and Opportunities for High-Speed Transport Aircraft," NASA CP-10003, Nov. 1987.

3. McElroy, M.B. and McConnell, J.C., "Nitrous Oxide: A Natural Source of Stratospheric NO," Journal of the Atmospheric Sciences, Vol. 28, Sept. 1971, pp. 1095-1098.

4. Broderick, A.J. and Krull, N.P., "Considerations of High Altitude Emissions," NASA CP-001-PT-2, 1976, pp. 565-574.

5. Grobecker, A.J., Coronite, S.C., and Cannon, R.H., Jr., "Report of Findings: The Effects of Stratospheric Pollution by Aircraft," Department of Transportation Report DOT-TST-75-50, 1974.

6. Nuessle, V.D. and Holcomb, R.W., "Will the SST Pollute the Stratosphere?" Science, Vol. 168, June 26, 1970, pp. 1562.

7. Broderick, A.J., English, J.M., and Forney, A.K., "An Initial Estimate of Aircraft Emissions in the Stratosphere in 1990," AIAA Paper 73-508, June 1973.

8. Environmental Impact of Stratospheric Flight, Climatic Impact Committee, National Academy of Sciences, Washington, D.C., 1975.

9. Hidalgo, H., "The Stratosphere, Perturbed by Propulsion Effluents," U.S. Department of Transportation, Washington, D.C., Appendix E, Summary-CIAP Mon.3, DOT-TST-75-53, Dec. 1974.

10. Oliver, R.C., Bauer, E., Hidalgo, H., Gardner, K.A., and Wasylkiwskyj, W., "Aircraft Emissions: Potential Effects on Ozone and Climate, A Review and Progress Report," Federal Aviation Administration, FAA-EQ-77-3, Mar. 1977.

11. Novick, A.S. and Troth, D.L., "Low NO_x Heavy Fuel Combustor Concept Program," NASA CR-165367, Oct. 1981.

12. Lister, E., Niedzwiecki, R.W., and Nichols, L., "Low NO_x Heavy Fuel Combustor Program," ASME Paper 80-GT-69, Mar. 1980.

13. Pierce, R.M., Smith, C.E., and Hinton, B.S., "Low NO_x Combustor Development for Stationary Gas Turbine Engines," Proceedings of the Third Stationary Source Combustion Symposium, EPA-600/7-70-050C, Vol. III, Feb. 1979.

14. Bittker, D.A. and Wolfbrandt, G., "Effect of Fuel Nitrogen and Hydrogen Content on Emissions in Hydrocarbon Combustion," NASA TM-81612, 1981.

15. Takagi, T., Tatsumi, T., and Ogasawara, M., "Nitric Oxide Formation from Fuel Nitrogen in Staged Combustion: Roles of HCN and NH_i," Combustion and Flame, Vol. 35, May 1979, pp. 17-25.

16. Niedzwiecki, R.W., Juhasz, A.J., and Anderson, D.N., "Performance of a Swirl Can Primary Combustor to Outlet Temperatures of 3600 °F (2256 K)," NASA TM X-52902, 1970.

17. Niedzwiecki, R.W., "The Experimental Clean Combustor Program - Description and Status to November 1975," NASA TM X-71849, 1975.

18. Niedzwiecki, R.W. and Jones, R.E., "Pollution Measurements of a Swirl-Can Combustor," NASA TM X-68160, 1972.

19. Gleason, C.C. and Bahr, D.W., "The Experimental Clean Combustor Program, Phase III: Final Report," NASA CR-135384, 1978.

20. Roberts, R., Fiorentino, A. and Greene, W., "Experimental Clean Combustor Program, Phase III: Final Report," NASA CR-135253, 1977.

21. Rudey, R.A. and Reck, G.M., "Advanced Combustion Techniques for Controlling NO_x Emissions of High Altitude Cruise Aircraft," NASA TM X-73473, 1976.

22. Roffe, G. and Antonio, F., "Effect of Premixing Quality on Oxides of Nitrogen in Gas Turbine Combustors," NASA CR-2657, 1976.

23. Roffe, G., "Effect of Inlet Temperature and Pressure on Emissions from a Premixing Gas Turbine Primary Zone Combustor," NASA CR-2740, 1976.

24. Anderson, D.N., "Emissions of Oxides of Nitrogen from an Experimental Premixed-Hydrogen Burner," NASA TM X-3393, 1976.

25. Heywood, J.B. and Mikus, T., "Parameters Controlling Nitric Oxides Emissions from Gas Turbine Combustors," Atmospheric Pollution by Aircraft Engines, Apr. 1973.

26. Anderson, D.N., "Effect of Hydrogen Injection on Stability and Emissions of an Experimental Premixed Prevaporized Propane Burner," NASA TM X-3301, 1975.

27. Shaw, H., "The Effects of Water, Pressure and Equivalence Ratio on Nitric Oxide Production in Gas Turbines," Journal of Engineering for Power, Vol. 96, July 1974, pp. 240-246. (ASME 73-WA/GT-1-74A13292.)

28. Radhakrishnan, K. and Bittker, D.A., "GCKP86--An Efficient Code for General Chemical Kinetics and Sensitivity Analysis Computations," Eastern Section, Combustion Institute Fall Meetings 15-17, Dec. 1986, pp. 46-1 to 46-4.

29. Radhakrishnan, K. and Bittker, D.A., "LSENS - General Kinetics and Sensitivity Analysis Program for Efficient Chemical Kinetics and Sensitivity Analysis Computations," (proposed NASA Technical Paper).

30. Hanson, R.K. and Salimian, S., "Survey of Rate Constants in the N/H/O system," Combustion Chemistry, Springer Verlag, 1984, pp. 361-421.

31. Warnatz, J., "Rate Coefficients in the C/H/O System," in Combustion Chemistry, Springer Verlag, 1984, pp. 197-360.

32. Westley, F., "Table of Recommended Rate Constants for Chemical Reactions Occurring in Combustion," National Bureau of Standards, NSRDS-NBS 67, Apr. 1980.

33. Peterson, R.C. and Laurendau, N.M., "Kinetic Mechanism for Fuel-Nitrogen Conversion in Lean to Rich Flames," Combustion Institute, Central States Section Paper CSS/CI82-15, 1982.

34. Brabbs, T.A., Lezberg, E.A., Bittker, D.A., and Robertson, T.F., "Hydrogen Oxidation Mechanism with Applications to (1) the Chaperon Efficiency of CO_2 and (2) Vitiated Air Testing," NASA TM-100186, 1987.

35. Westley, F., Herron, J.T., and Cvetanovic, R.J., "Compilation of Chemical Kinetic Data for Combustion Chemistry," Part 1, National Bureau of Standards, NSRDS-NBS 73, Aug. 1987.

36. Wakelyn, N.T., Jachimowski, C.J., and Wilson, C.H., "Experimental and Analytical Study of Nitric Oxide Formation During Combustion of Propane in a Jet-Stirred Combustor," NASA TP-1181, May 1978.

37. Miller, J.A., Mitchel, R.E., Smooke, M.D., and Kee, R., "Toward a Comprehensive Chemical Kinetic Model for the Oxidation of Acetylene," 19th International Symposium on Combustion, 1983, pp. 181-96.

38. Jachimowski, C.J., "Experimental and Analytical Study of Acetylene and Ethylene Oxidation Behind Shock Waves," Combustion and Flame, Vol. 29, 1977, pp. 55-56.

39. Westbrook, C.K. and Dryer, F.L., "Chemical Kinetic Modeling of Hydrocarbon Combustion," Progress in Energy and Combustion Science, Vol. 10, 1984, pp. 1-57.

40. Brabbs, T.A. and Brokaw, R.S., "Shock Tube Measurements of Specific Reaction Rates in the Branched Chain CH_4-CO-O_2 System," 15th International Symposium on Combustion, 1975, pp. 893-901.

41. Olson, D.B. and Gardner, W., "Combustion of Methane in Fuel Rich Mixtures," Combustion and Flame, Vol. 32, June 1978, pp. 151-61.

42. Schultz, D.F. and Wolfbrandt, G., "Flame Tube Parametric Studies for Control of Fuel Bound Nitrogen Using Rich-Lean Two-Stage Combustion," NASA TM-81472, 1980.

TABLE I. - CHARACTERISTICS OF CRUISE OPERATING CONDITIONS FOR SUBSONIC VERSUS HSCT AIRCRAFT SYSTEMS

[Standard day conditions.]

Condition	Subsonic production turbofan, P&WA JT9D-7	Supersonic Concorde afterburning turbojet, Olympus 593	Supersonic HSCT
Fuel	JP	JP	JP
Cruise altitude, km	10.7	17.7	17.7
Cruise Mach number	0.85	2.0	2.0
Compressor discharge airflow rate, kg/sec	51.5	83.0	65.0
Combustor inlet temperature, K	710	824	1073
Combustor inlet pressure, atm	9.7	6.5	16.8
Combustor exit temperature, K	1410	1320	2510
Fuel-air ratio	0.018	0.0141	0.053
Fuel flow rate, kg/sec	0.78	1.17	2.67
Estimated cruise NO_x emission, g NO_2/kg fuel	16 to 23	18 to 19	60 to 89
Certification year	1971	1976	2010

TABLE 2. - PROPANE-AIR COMBUSTION AND NO_x CHEMICAL KINETIC MODEL

Reaction number	Reaction	Rate constant[a,b]			Reference
		A	n	E_a	
1	$NO + O = N + O_2$	3.8×10^{9}	1	41 370	30
2	$O + N_2 = NO + N$	1.82×10^{14}	0	76 250	30
3	$NO + H = N + OH$	2.63×10^{14}	0	50 410	30
4	$CH + N_2 = HCN + N$	1.0×10^{11}	0	19 000	32
5	$CH + NO = N + HCO$	1.6×10^{13}	0	9 940	32
6	$CH + NO = O + HCN$	2.0×10^{12}	0	0	32
7	$CN + H_2 = HCN + H$	6.0×10^{13}	0	5 300	14
8	$O + HCN = OH + CN$	1.4×10^{11}	.68	16 900	14
9	$OH + HCN = HNCO + H$	4.0×10^{11}	0	2 800	33
10	$CN + O = CO + N$	1.2×10^{13}	0	0	33
11	$CN + OH = NCO + H$	2.5×10^{14}	0	6 000	33
12	$H_2 + NCO = HNCO + H$	1.0×10^{14}	0	9 000	33
13	$HNCO + H = NH_2 + CO$	1.0×10^{14}	0	8 500	33
14	$CN + O_2 = NCO \bullet O$	3.2×10^{13}	0	1 000	33
15	$CN + CO_2 = NCO + CO$	3.7×10^{12}	0	0	33
16	$O + NCO = NO + CO$	2.0×10^{13}	0	0	33
17	$N + NCO = N_2 + CO$	1.0×10^{13}	0	0	33
18	$H + NCO = NH + CO$	2.0×10^{13}	0	0	33
19	$NH + OH = N + H_2O$	5.0×10^{11}	.5	2 000	30
20	$HO_2 + NO = NO_2 + OH$	2.09×10^{12}	0	-477	30
21	$O + NO_2 = NO + O_2$	1.0×10^{13}	0	596	30
22	$NO + O = NO_2 + M$	5.62×10^{15}	0	-1 160	14
23	$NO_2 + H = NO + OH$	3.47×10^{14}	0	1 470	34
24	$N + NO_2 = 2NO$	4.0×10^{12}	0	0	30
25	$M + N_2O = N_2 + O$	6.92×10^{23}	-2.5	65 000	30
26	$O + N_2O = N_2 + O_2$	1.0×10^{14}	0	28 020	30
27	$O + N_2O = 2NO$	6.92×10^{13}	0	26 630	30
28	$N_2O + H = N_2 + OH$	7.59×10^{13}	0	15 100	30
29	$NO_2 + H_2 = HNO_2 + H$	2.4×10^{13}	0	29 000	34
30	$OH + NO_2 = HNO_3 + M$	3.0×10^{15}	0	-3 800	34
31	$OH + NO = HNO_2 + M$	5.6×10^{15}	0	-1 700	34
32	$HNO + H = H_2 + NO$	5.0×10^{12}	0	0	34
33	$H + NO = HNO + M$	5.4×10^{15}	0	-600	34
34	$HNO + OH = H_2O + NO$	3.6×10^{13}	0	0	34
35	$C_3H_8 = C_2H_5 + CH_3$	5.0×10^{15}	0	83 500	31
36	$CH_3 + C_3H_8 = CH_4 + C_3H_7$	3.55×10^{12}	0	10 300	31
37	$C_3H_7 = C_2H_4 + CH_3$	3.0×10^{14}	0	33 200	31
38	$CH_3 + CH_3 = C_2H_6$	2.4×10^{14}	-.4	0	31
39	$H + C_2H_6 = C_2H_5 + H_2$	1.32×10^{14}	0	9 700	31
40	$O + C_2H_6 = C_2H_5 + OH$	1.13×10^{14}	0	7 850	35
41	$OH + C_2H_6 = C_2H_5 + H_2O$	1.45×10^{13}	0	3 520	35
42	$M + C_2H_5 = C_2H_4 + H$	1.0×10^{17}	0	31 000	31
43	$C_2H_5 + O_2 = C_2H_4 + HO_2$	2.0×10^{12}	0	5 000	31
44	$H + C_2H_5 = C_2H_4 + H_2$	4.8×10^{13}	0	0	31
45	$CH_3 + CH_2 = C_2H_4 + H$	2.0×10^{13}	0	0	31
46	$H + C_2H_4 = H_2 + C_2H_3$	1.5×10^{14}	0	10 200	31
47	$M + C_2H_4 = C_2H_2 + H_2$	2.6×10^{17}	0	79 300	31
48	$C_2H_4 + OH = C_2H_3 + H_2O$	1.0×10^{14}	0	3 500	36
49	$C_2H_4 + O = CH_3 + HCO$	2.26×10^{13}	0	2 700	36
50	$C_2H_4 + O = CH_2O + CH_2$	2.5×10^{13}	0	5 000	36

[a]Rate constant as given by $k = AT^n \exp(-E_a/RT)$, where T is temperature in K, and E_a is the reaction activation energy in cal/mol.

[b]Units of k are sec^{-1} for a unimolecular reaction, $cm^3/mol\text{-}sec$ for a bimolecular reaction, and $cm^6/mol^2\text{-}sec$ for a trimolecular reaction.

TABLE 2. - Concluded.

Reaction number	Reaction	Rate constant[a,b]			Reference
		A	n	E_a	
51	$M + C_2H_3 = C_2H_2 + H$	3.0×10^{16}	0	40 500	36
52	$C_2H_3 + O_2 = C_2H_2 + HO_2$	1.58×10^{13}	0	10 000	37
53	$C_2H_3 + H = C_2H_2 + H_2$	6.0×10^{12}	0	0	37
54	$C_2H_3 + OH = C_2H_2 + H_2O$	5.0×10^{12}	0	0	37
55	$M + C_2H_2 = C_2H + H$	1.0×10^{14}	0	114 000	38
56	$C_2H_2 + O = CH_2 + CO$	5.2×10^{13}	0	3 700	38
57	$C_2H_2 + O = C_2H + OH$	3.2×10^{15}	-.6	17 000	38
58	$C_2H_2 + O = C_2HO + H$	3.56×10^{4}	2.7	1 390	39
59	$C_2HO + CH_2 = C_2H_3 + CO$	3.0×10^{13}	0	0	39
60	$C_2HO + CH_2 = CH_2O + C_2H$	1.0×10^{13}	0	2 000	37
61	$C_2H_2 + OH = C_2H + H_2O$	6.0×10^{12}	0	7 000	38
62	$C_2H_2 + O_2 = 2HCO$	4.0×10^{12}	0	28 000	39
63	$C_2H + O2 = HCO + CO$	1.0×10^{13}	0	7 000	39
64	$C_2H + O = CO + CH$	1.4×10^{13}	0	3 150	31
65	$H + CH_4 = CH_3 + H_2$	1.26×10^{14}	0	11 900	40
66	$O + CH_4 = CH_3 + OH$	1.9×10^{14}	0	11 720	40
67	$OH + CH_4 = CH_3 + H_2O$	2.5×10^{13}	0	5 010	40
68	$CH_3 + OH = CH_2O + H_2$	7.4×10^{12}	0	0	31
69	$CH_3 + OH = CH_3O + H$	6.3×10^{12}	0	0	35
70	$M + CH_3 = CH_2 + H$	1.95×10^{16}	0	91 600	39
71	$CH_3 + O = CH_2O + H$	1.29×10^{14}	0	2 000	39
72	$CH_3 + O_2 = CH_3O + O$	2.4×10^{13}	0	28 680	40
73	$M + CH_3O = CH_2O + H$	5.0×10^{13}	0	21 000	39
74	$M + CH_2O = HCO + H$	5.0×10^{16}	0	81 000	39
75	$CH_2O + OH = HCO + H_2O$	5.0×10^{15}	0	13 000	41
76	$CH_2O + H = HCO + H_2$	2.0×10^{13}	0	3 300	41
77	$CH_2O + O = HCO + OH$	5.0×10^{13}	0	4 600	41
78	$HCO + O = CO + OH$	3.0×10^{13}	0	0	41
79	$HCO + OH = CO + H_2O$	3.0×10^{13}	0	0	41
80	$HCO + H = CO + H_2$	2.0×10^{13}	0	0	41
81	$HCO + O_2 = CO + HO_2$	3.0×10^{13}	0	0	31
82	$M + HCO = H + CO$	2.9×10^{14}	0	15 570	14
83	$CO + O = CO_2 + M$	2.4×10^{15}	0	4 100	35
84	$CO + O_2 = CO_2 + O$	2.5×10^{12}	0	47 690	35
85	$CO + OH = CO_2 + H$	4.17×10^{11}	0	1 000	34
86	$H + O_2 = OH + O$	1.66×10^{14}	0	16 400	34
87	$O + H_2 = OH + H$	3.26×10^{13}	0	9 800	34
88	$O + H_2O = OH + OH$	6.76×10^{13}	0	18 360	34
89	$H_2 + OH = H_2O + H$	2.1×10^{13}	0	5 100	34
90	$H + O_2 = HO_2 + M$	2.0×10^{18}	-1	0	34
91	$H + OH = H_2O + M$	2.17×10^{22}	-2	0	14
92	$H + H = H_2 + M$	6.4×10^{17}	-1	0	14
93	$O + O = O_2 + M$	1.91×10^{13}	0	-1 790	14
94	$H + CH_3 = H_2 + CH_2$	2.7×10^{11}	.67	25 700	14
95	$O + CH_3 = OH + CH_2$	1.9×10^{11}	.68	25 700	14
96	$OH + CH_3 = H_2O + CH_2$	2.7×10^{11}	.67	25 700	14
97	$CH + CO_2 = HCO + CO$	3.7×10^{12}	0	0	14
98	$CH + O_2 = HCO + O$	1.0×10^{13}	0	0	14
99	$CH_2 + O_2 = CH_2O + O$	5.0×10^{11}	.5	6 960	35
100	$CH_2 + O = CH + OH$	2.0×10^{11}	.7	25 800	35
101	$CH_2 + OH = CH + H_2O$	5.0×10^{11}	.5	5 960	35
102	$CH_2 + H = CH + H_2$	3.2×10^{11}	.7	4 970	35

[a]Rate constant as given by $k = AT^n \exp(-E_a/RT)$, where T is temperature in K, and E_a is the reaction activation energy in cal/mol.

[b]Units of k are sec^{-1} for a unimolecular reaction, cm^3/mol-sec for a bimolecular reaction, and cm^6/mol^2-sec for a trimolecular reaction.

TABLE 3. - THIRD-BODY COLLISION REACTIONS AND CHAPERON EFFICIENCY

Third-body reactions	Third-body species	Chaperon efficiency factor
$H + O_2 = HO_2 + M$	O_2	1.3
	N_2	1.3
$H + O_2 = HO_2 + M$	H_2O	21.3
	CO_2	7.0
$H + O_2 = HO_2 + M$	CO	2.0
	CH_4	5.0
$H + O_2 = HO_2 + M$	H_2	5.0
$H + OH = H_2O + M$	H_2O	6.5
$H + OH = H_2O + M$	CO_2	2.0
$H + OH = H_2O + M$	CO	1.6
$OH + NO_2 = HNO_3 + M$	O_2	.7
	H_2	1.4

TABLE 4. - RICH BURN/QUICK QUENCH/LEAN BURN COMBUSTOR NO_x EMISSIONS PARAMETRIC DATA: PRIMARY-ZONE EQUIVALENCE RATIO, INLET AIR TEMPERATURE

[Initial pressure, 7.6 atm; primary-zone residence time, ≈3 msec; secondary-zone residence time, ≈2 msec.]

Inlet air temperature, K	Primary-zone equivalence ratio									
	0.6	0.8	0.9	1.0	1.2	1.4	1.6	1.8	1.9	2.0
	NO_x emissions, ppmm									
1000	438	1329	1895	2175	1233	293	157	178	195	205
1100	459	1948	2590	2793	1603	463	222	274	316	334
1200	733	2792	3434	3488	2027	731	424	445	512	566
1311	1228	4012	4519	4340	2620	1204	777	777	840	936

TABLE 5. - RICH BURN/QUICK QUENCH/LEAN BURN COMBUSTOR CO EMISSIONS PARAMETRIC DATA: PRIMARY-ZONE EQUIVALENCE RATIO, INLET AIR TEMPERATURE

[Initial pressure, 7.6 atm; primary-zone residence time, ≈3 msec; secondary-zone residence time, ≈2 msec.]

Inlet air temperature, K	Primary-zone equivalence ratio									
	0.6	0.8	0.9	1.0	1.2	1.4	1.6	1.8	1.9	2.0
	CO emissions, ppmm									
1000	137	142	158	229	449	807	1184	1496	1627	1716
1100	160	174	199	262	481	836	1136	1489	1677	1748
1200	71	221	266	307	549	878	1222	1499	1607	1768
1311	76	304	343	409	717	1039	1281	1506	1616	1760

TABLE 6. - RICH BURN/QUICK QUENCH/LEAN BURN COMBUSTOR CO_2 EMISSIONS PARAMETRIC DATA: PRIMARY-ZONE EQUIVALENCE RATIO, INLET AIR TEMPERATURE

[Initial pressure, 7.6 atm; primary-zone residence time, ≈3 msec; secondary-zone residence time, ≈2 msec.]

Inlet air temperature, K	Primary-zone equivalence ratio									
	0.6	0.8	0.9	1.0	1.2	1.4	1.6	1.8	1.9	2.0
	CO_2 emissions, ppmm									
1000	74 631	72 505	71 844	71 454	71 766	72 680	75 888	80 416	82 301	83 329
1100	49 782	71 259	70 707	70 539	71 571	72 234	74 410	78 378	80 584	82 125
1200	49 020	70 067	69 662	69 842	71 788	72 480	73 326	76 474	78 579	80 476
1311	48 045	68 820	68 737	69 389	72 504	73 392	73 112	74 905	76 598	78 486

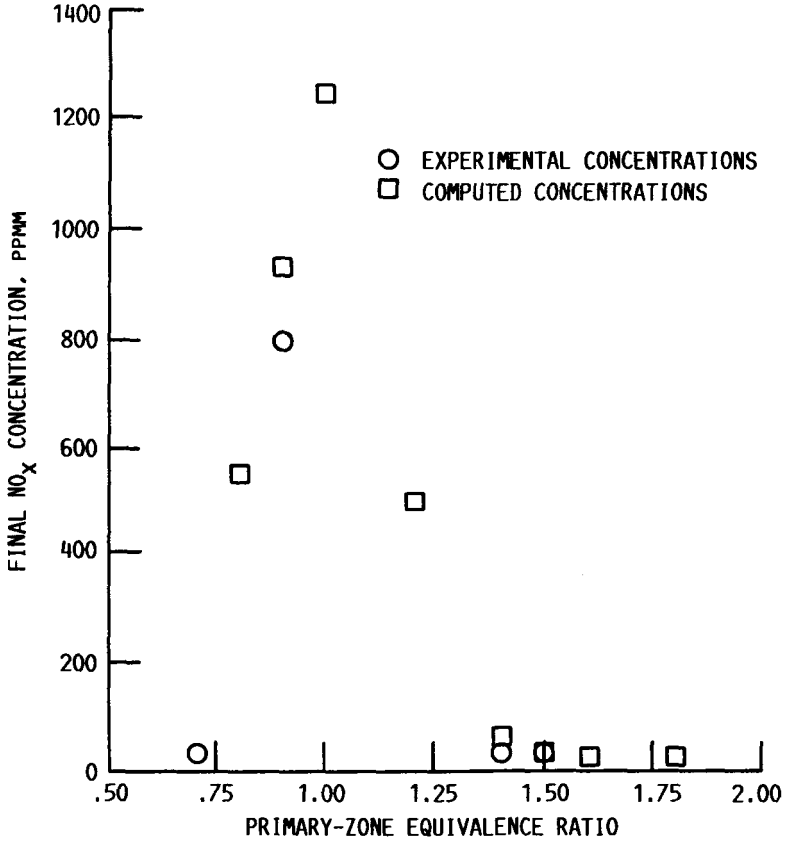

FIG. 1 COMPARISON OF COMPUTED AND EXPERIMENTAL NO_x CONCENTRATIONS. INLET AIR TEMPERATURE, 672 K, INITIAL PRESSURE, 5 ATM; PRIMARY-ZONE RESIDENCE TIME, 11 MSEC; SECONDARY-ZONE EQUIVALENCE RATIO, 0.5; SECONDARY-ZONE RESIDENCE TIME, 2 MSEC.

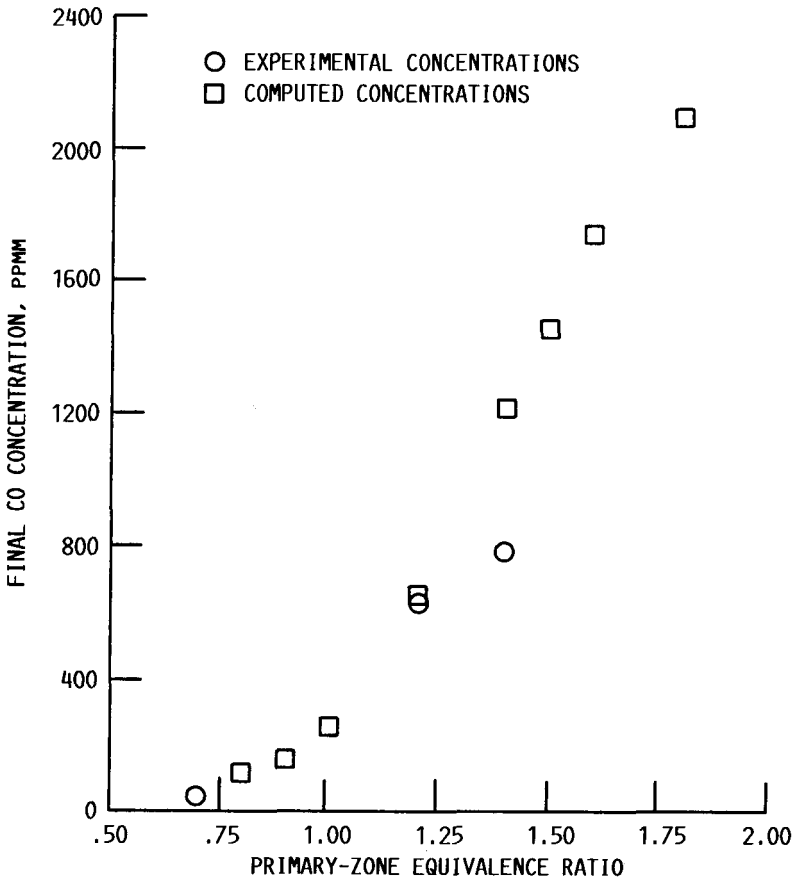

FIG. 2 COMPARISON OF COMPUTED AND EXPERIMENTAL CO CONCENTRATIONS. INLET AIR TEMPERATURE, 672 K; INITIAL PRESSURE, 5 ATM; PRIMARY-ZONE RESIDENCE TIME, 11 MSEC; SECONDARY-ZONE EQUIVALENCE RATIO, 0.5; SECONDARY-ZONE RESIDENCE TIME, 2 MSEC.

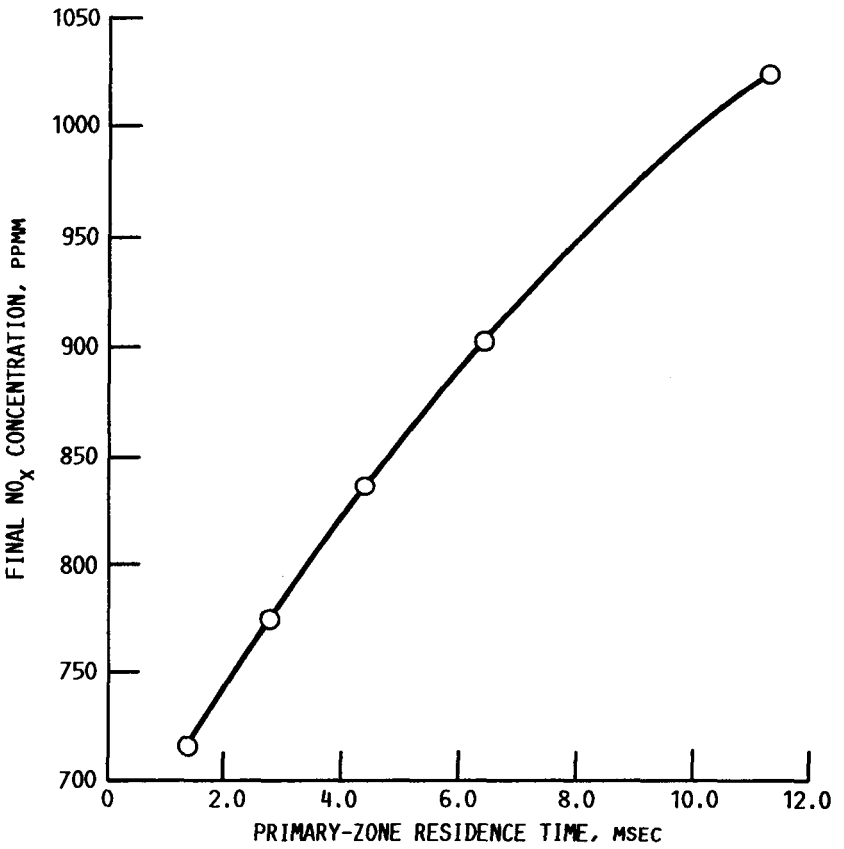

FIG. 3 EFFECT OF PRIMARY-ZONE RESIDENCE TIME ON NO_x EMISSION. PRIMARY-ZONE EQUIVALENCE RATIO, 1.6; INLET AIR TEMPERATURE, 1311 K; INITIAL PRESSURE, 7.6 ATM.

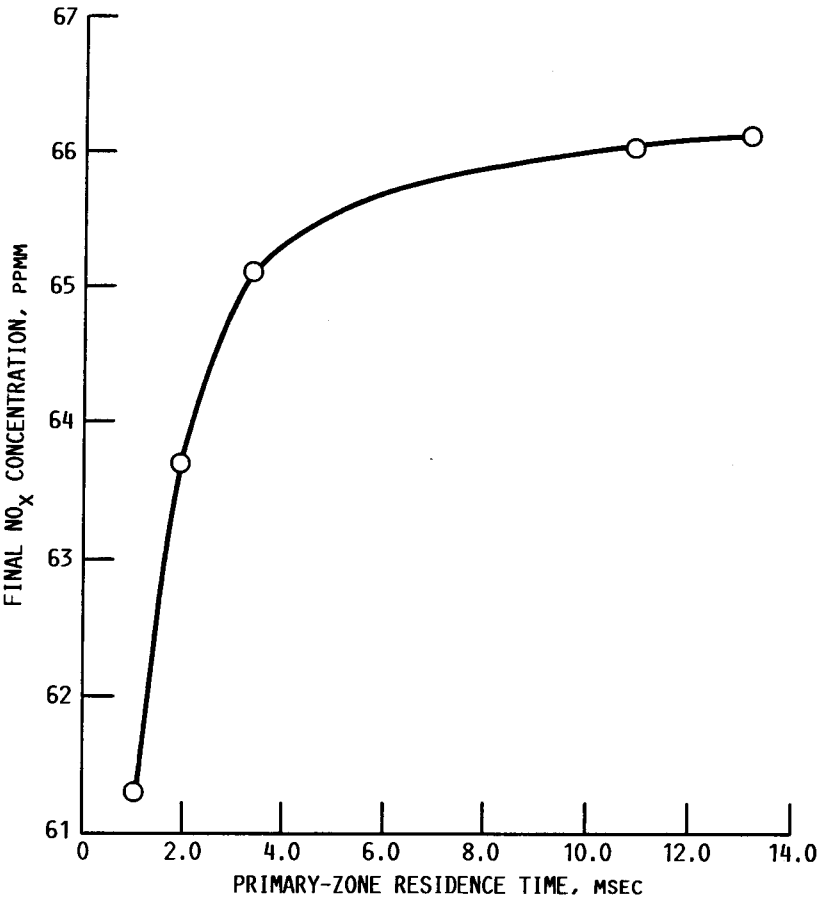

FIG. 4 EFFECT OF PRIMARY-ZONE RESIDENCE TIME ON NO_x EMISSION. PRIMARY-ZONE EQUIVALENCE RATIO, 1.4; INLET AIR TEMPERATURE, 672 K; INITIAL PRESSURE, 5 ATM.

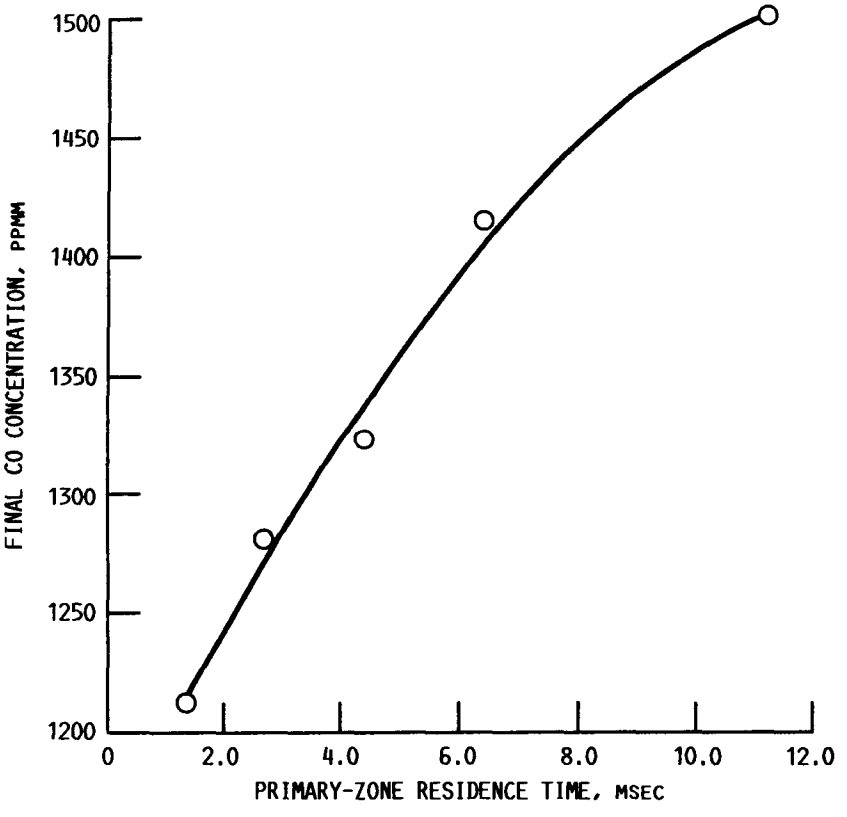

FIG. 5 EFFECT OF PRIMARY-ZONE RESIDENCE TIME ON CO EMISSION. PRIMARY-ZONE EQUIVALENCE RATIO, 1.6; INLET AIR TEMPERATURE, 1311 K; INITIAL PRESSURE, 7.6 ATM.

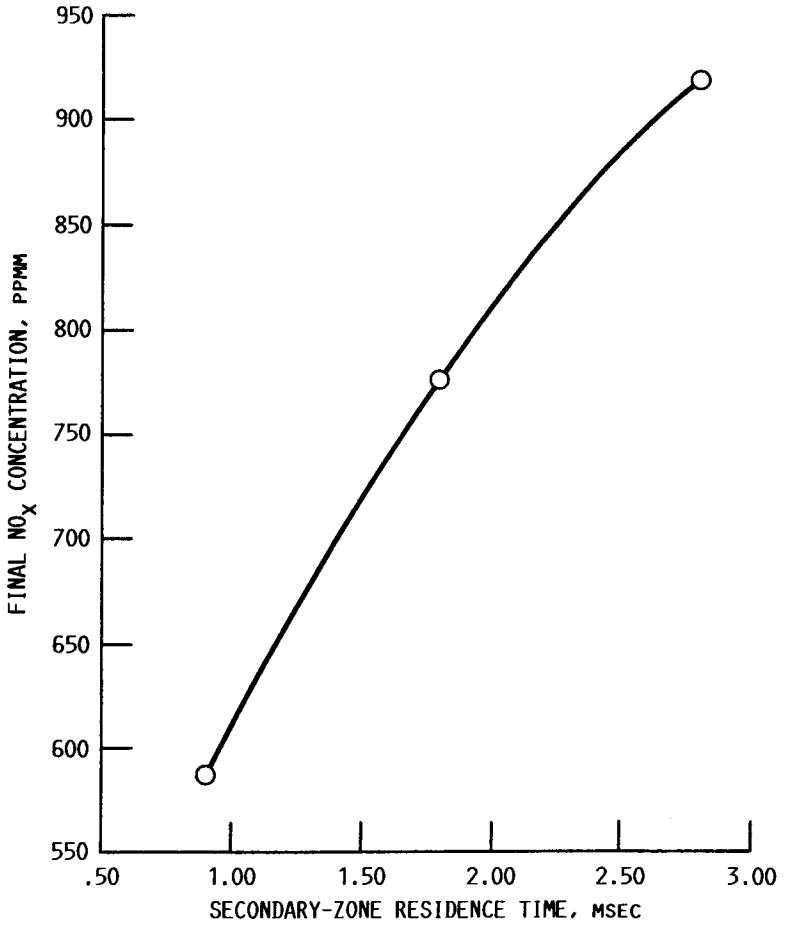

FIG. 6 EFFECT OF LEAN SECONDARY-ZONE RESIDENCE TIME ON NO_x EMISSION. PRIMARY-ZONE EQUIVALENCE RATIO, 1.6; INLET AIR TEMPERATURE, 1311 K; INITIAL PRESSURE, 7.6 ATM.

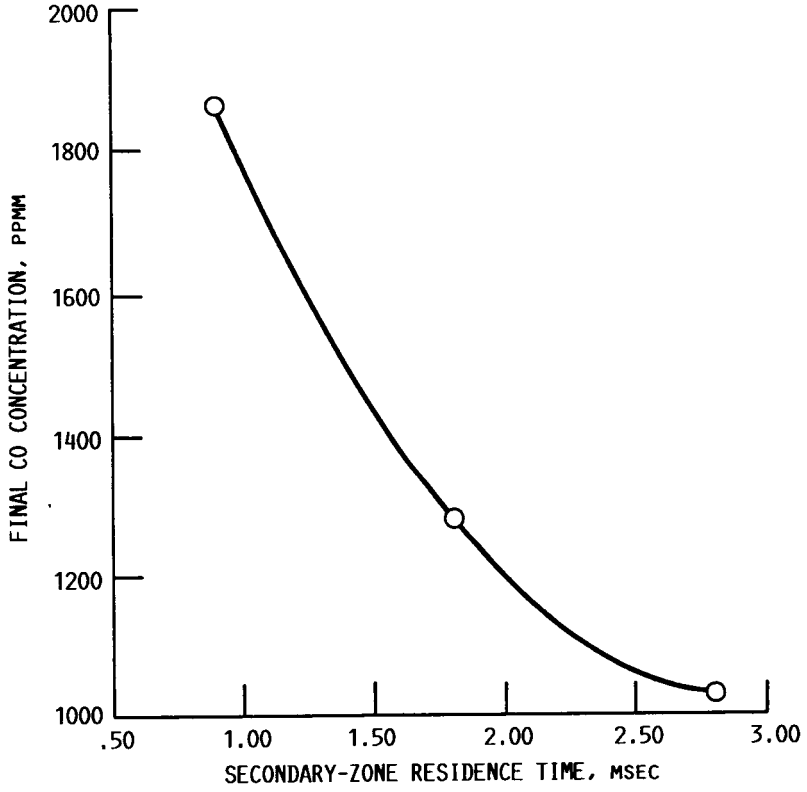

FIG. 7 EFFECT OF LEAN SECONDARY-ZONE RESIDENCE TIME ON CO EMISSION. PRIMARY-ZONE EQUIVALENCE RATIO, 1.6; INLET AIR TEMPERATURE, 1311 K; INITIAL PRESSURE, 7.6 ATM.

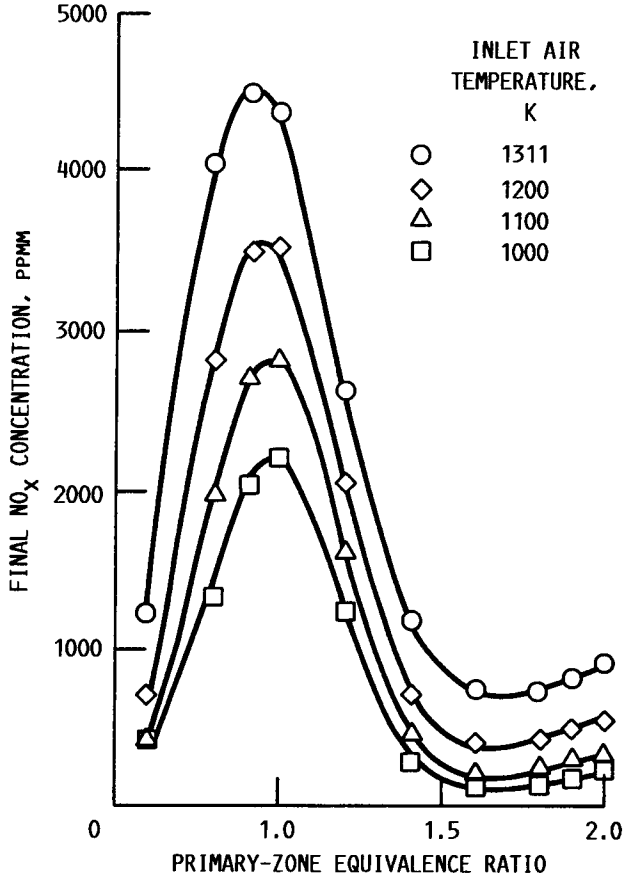

FIG. 8 EFFECT OF PRIMARY-ZONE EQUIVALENCE RATIO ON FINAL NO_x CONCENTRATION FOR VARIOUS INLET AIR TEMPERATURES. INITIAL PRESSURE, 7.6 ATM.

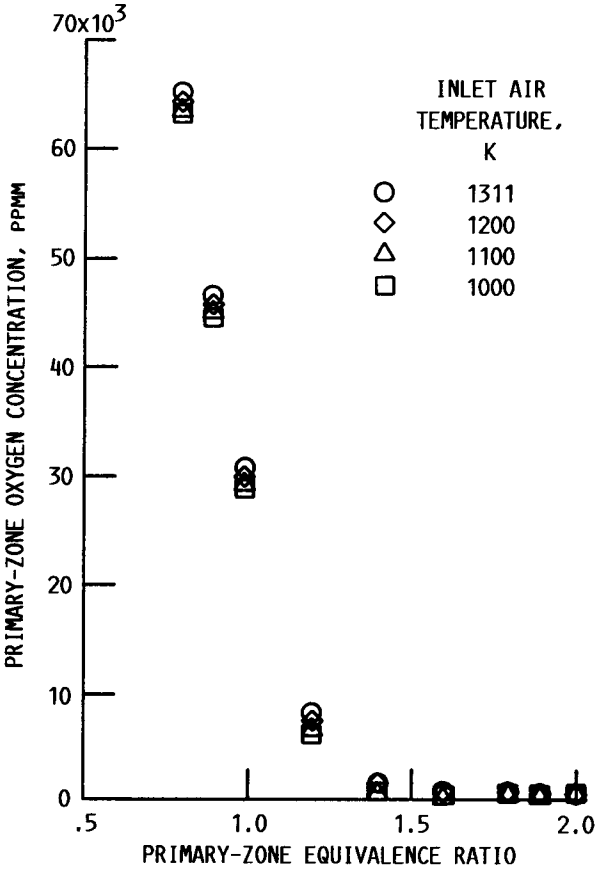

FIG. 9 EFFECT OF PRIMARY-ZONE EQUIVALENCE RATIO ON COMPUTED PRIMARY-ZONE OXYGEN CONCENTRATION FOR VARIOUS INLET AIR TEMPERATURES. INITIAL PRESSURE, 7.6 ATM.

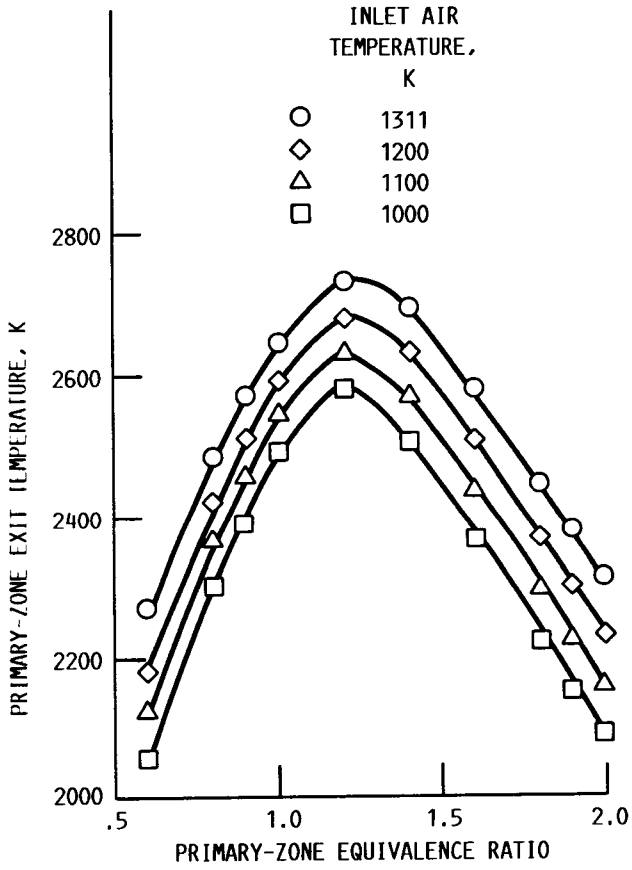

FIG. 10. - EFFECT OF PRIMARY-ZONE EQUIVALENCE RATIO ON PRIMARY-ZONE EXIT TEMPERATURE FOR VARIOUS INLET AIR TEMPERATURES. INLET PRESSURE, 7.6 ATM.

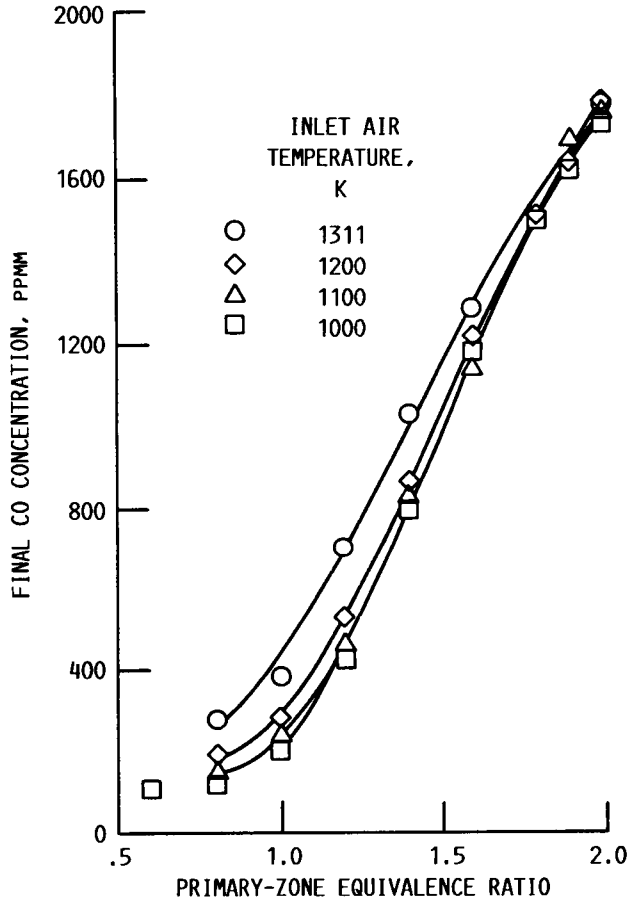

FIG. 11 EFFECT OF PRIMARY-ZONE EQUIVALENCE RATIO ON FINAL CO CONCENTRATION FOR VARIOUS INLET AIR TEMPERATURES. INITIAL PRESSURE, 7.6 ATM.

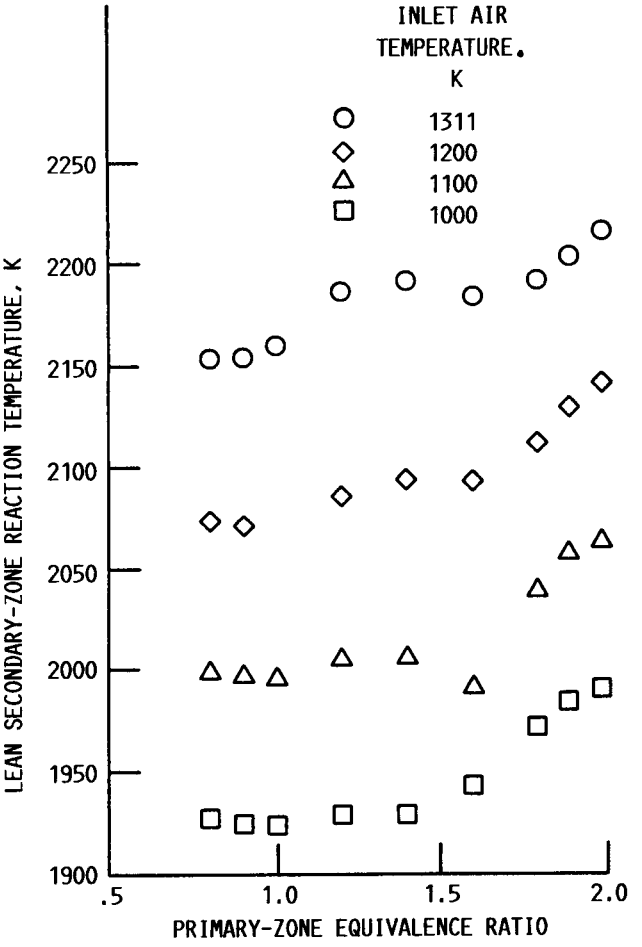

FIG. 12 EFFECT OF PRIMARY-ZONE EQUIVALENCE RATIO ON LEAN SECONDARY-ZONE REACTION TEMPERATURE FOR VARIOUS INLET AIR TEMPERATURES. INITIAL PRESSURE, 7.6 ATM.

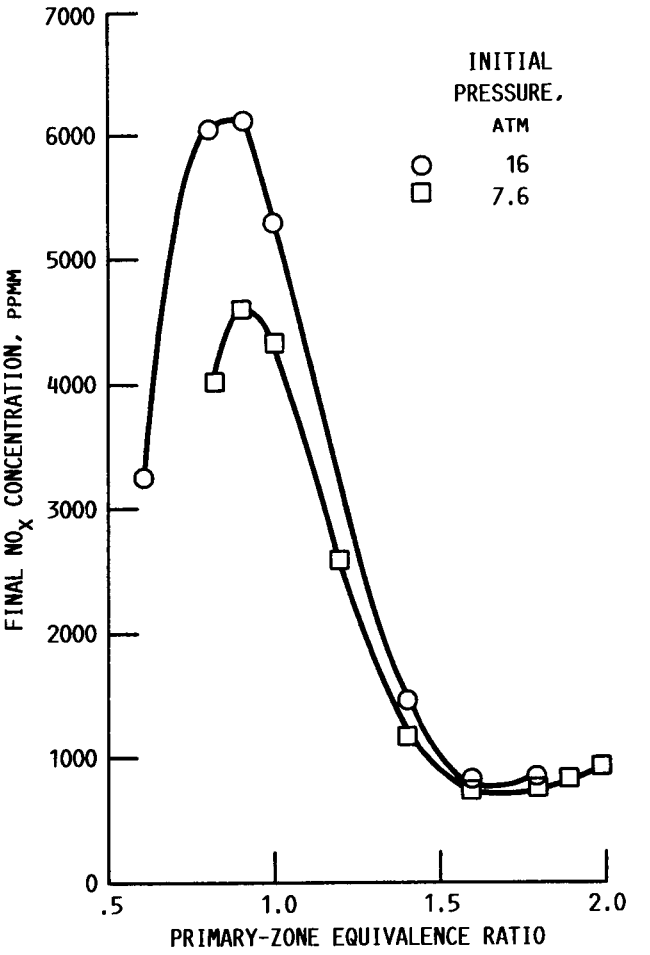

FIG. 13 EFFECT OF PRESSURE ON NO_x EMISSION. INLET AIR TEMPERATURE, 1311 K; SECONDARY-ZONE RESIDENCE TIME, 2 MSEC; SECONDARY-ZONE EQUIVALENCE RATIO, 0.5.

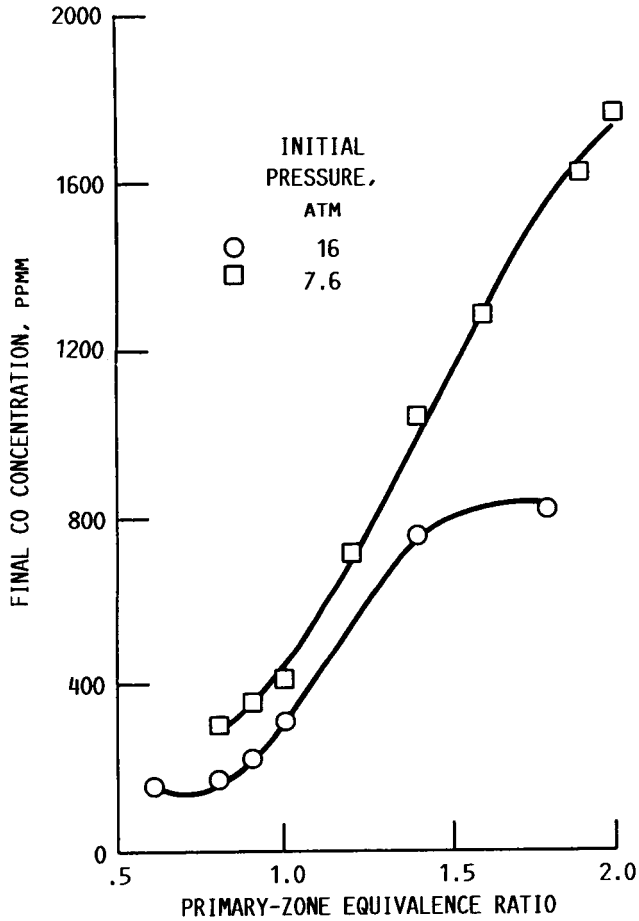

FIG. 14 EFFECT OF PRESSURE ON CO EMISSION. INLET AIR TEMPERATURE, 1311 K; SECONDARY-ZONE RESIDENCE TIME, 2 MSEC; SECONDARY-ZONE EQUIVALENCE RATIO, 0.5.

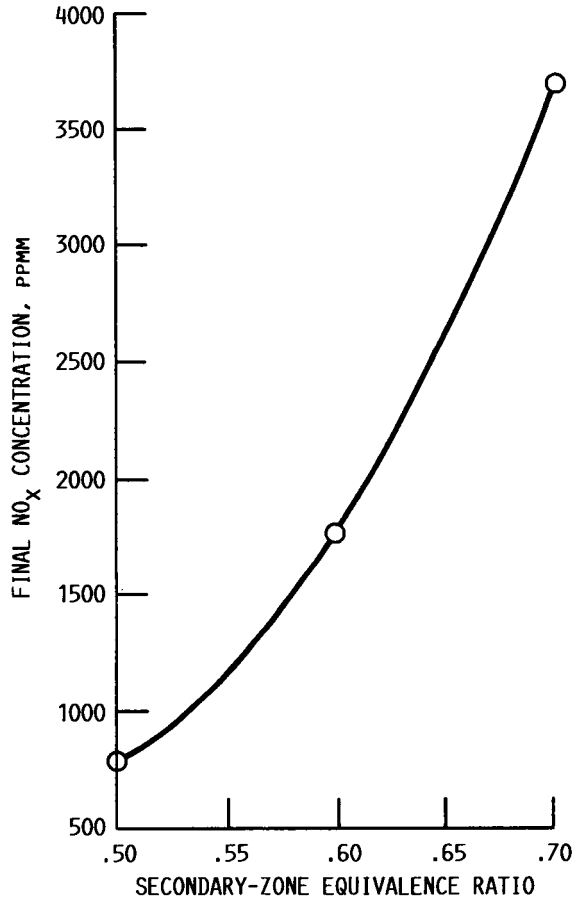

FIG. 15 EFFECT OF SECONDARY-ZONE EQUIVALENCE RATIO ON NO_x EMISSION. PRIMARY-ZONE EQUIVALENCE RATIO, 1.6; SECONDARY-ZONE RESIDENCE TIME, 2 MSEC; INLET AIR TEMPERATURE, 1311 K; INITIAL PRESSURE, 7.6 ATM.

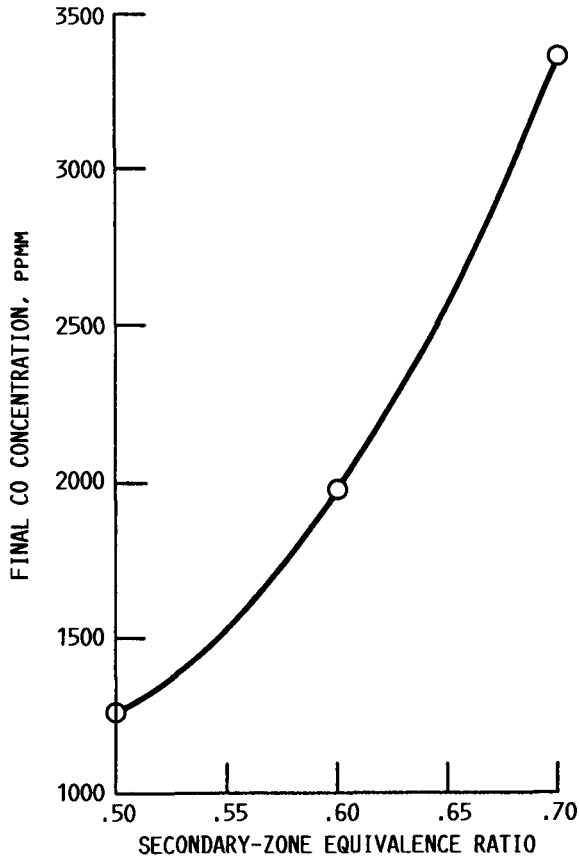

FIG. 16 EFFECT OF SECONDARY-ZONE EQUIVALENCE RATIO ON CO EMISSION. PRIMARY-ZONE EQUIVALENCE RATIO, 1.6; SECONDARY-ZONE RESIDENCE TIME, 2 MSEC; INLET AIR TEMPERATURE, 1133 K; INITIAL PRESSURE, 7.6 ATM.

NASA
National Aeronautics and Space Administration

Report Documentation Page

1. Report No.	2. Government Accession No.	3. Recipient's Catalog No.
NASA TM-101977 AIAA-89-2942		

4. Title and Subtitle

Investigation of Low NO_x Staged Combustor Concept in High-Speed Civil Transport Engines

5. Report Date

6. Performing Organization Code

7. Author(s)

Hung Lee Nguyen, David A. Bittker, and Richard W. Niedzwiecki

8. Performing Organization Report No.

E-4071

10. Work Unit No.

505-62-61

9. Performing Organization Name and Address

National Aeronautics and Space Administration
Lewis Research Center
Cleveland, Ohio 44135-3191

11. Contract or Grant No.

13. Type of Report and Period Covered

Technical Memorandum

12. Sponsoring Agency Name and Address

National Aeronautics and Space Administration
Washington, D.C. 20546-0001

14. Sponsoring Agency Code

15. Supplementary Notes

Prepared for the 25th Joint Propulsion Conference, cosponsored by the AIAA, ASME, SAE, and ASEE, Monterey, California, July 10-12, 1989.

16. Abstract

The purpose of this report is to predict levels of exhaust emissions due to high temperatures in the main combustor of High-Speed Civil Transport (HSCT) engines during supersonic cruise. These predictions are based on a new combustor design approach: a rich burn/quick quench/lean burn combustor. A two-stage stirred reactor model is used to calculate the combustion efficiency and exhaust emissions of this novel combustor. A propane-air chemical kinetics model is used to simulate the fuel-rich combustion of jet fuel. Predicted engine exhaust emissions are compared with available experimental test data. The effect of HSCT engine operating conditions on the levels of exhaust emissions is also presented. The work described in this paper is a part of the NASA Lewis Research Center High-Speed Civil Transport Low NO_x Combustor program.

17. Key Words (Suggested by Author(s))	18. Distribution Statement
Low No_x combustion; High speed civil transport; Rich burn/quick quench/lean burn; Lean premixed prevaporized	Unclassified – Unlimited Subject Category 07

19. Security Classif. (of this report)	20. Security Classif. (of this page)	21. No of pages	22. Price*
Unclassified	Unclassified	22	A03

NASA FORM 1626 OCT 86

*For sale by the National Technical Information Service, Springfield, Virginia 22161